

Freezing of a Long Liquid Column on the Texus-18 Sounding-Rocket Flight

Abstract A free-surface cylindrical column of water (86 mm long by 30 mm diameter) was established during the first minute of microgravity on a sounding-rocket flight. Cooling was applied at one of the supporting discs to permit the advance of the solidification front and free-surface deformation to be observed during the ensuing 5 min of microgravity. The solidification front remained planar and the free surface remained cylindrical throughout, until affected by re-entry deceleration.

Résumé Une colonne cylindrique d'eau à surface libre (86 mm par 30 mm de diamètre) s'est formée pendant la première minute de microgravité dans une fusée-sonde, et l'un des disques d'appui a été refroidi pour observer l'avance du front de solidification et la déformation à l'interface pendant les 5 minutes de microgravité qui restaient. Le front restait plat et la surface libre cylindrique pendant toute la durée du vol, jusqu'à ce que la décélération de la rentrée les perturbent.

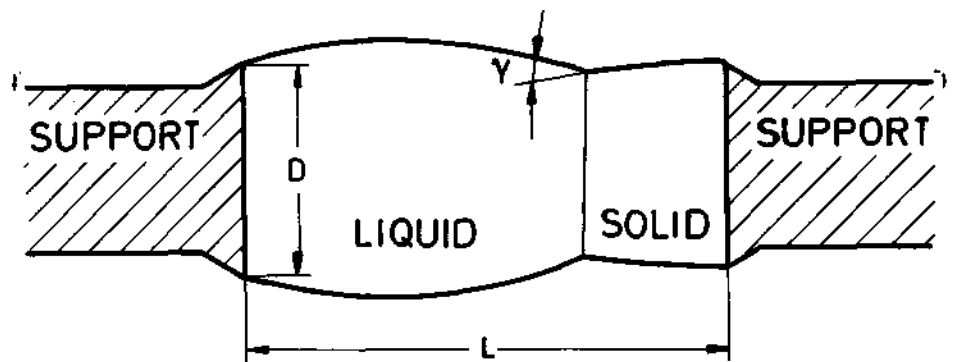
1. Introduction

A fluid-mechanical model of liquid-bridge equilibrium and stability had been successfully applied to the interpretation of two crystal-growth processes observed aboard Spacelab-1 in 1983: the resolidification of a silicon rod¹ and of a silicon sphere². This encouraged us to propose an experiment that would make it possible to examine some microscopic aspects of crystal growth by means of a simple model, namely that of the unidirectional freezing of a long column of liquid. The proposal was submitted to ESA in January 1986.

The main objective was to measure the so-called 'receding contact angle' γ on the solidification with a free surface (Fig. 1). The configuration shown in Figure 1 has many advantages; for example:

- The large size (86 mm compared with about 8 mm in conventional crystal growth by the floating-zone technique) makes the measurements easier and more precise.
- The mild ambient environment (freezing from ambient temperature instead of resolidifying a melt at near 2000 K) makes the conditioning and the diagnosis much simpler.
- The transparency of the liquid greatly assists the visualisation of residual motions induced by surface-tension gradients, front dynamics, g-jitter, and so on. Tracers were added to the liquid for this purpose.
- The chosen (near-critical) slenderness $[L/D=0.91(L/D)_{cr}]$ of the liquid bridge greatly enhances the sensitivity of this configuration to small residual forces.
- The chosen slenderness ($L/D=2.87$) is the same as that used in the experiments aboard Spacelab-D1 in 1985, although the columns are in this case slightly thinner because the Texas discs are 30 mm in diameter, instead of the 35 mm on Spacelab-D1).

Figure 1. Receding contact angle γ in the solidification with a free surface



2. Preparation of the flight experiment

Ground experiments were started early, with the main aim of selecting the working liquid. In principle, the idea was to initiate a unidirectional solidification process in a transparent liquid, either by solidification of an already molten solid of low melting temperature, or by freezing a room-temperature liquid. The substance required was to be readily available, transparent, nontoxic and nonflammable and have a well-defined melting point, low volatility (to avoid variations in liquid volume) and compatibility with the tracers (some liquids do not mix well with the solid 0.1 mm-diameter ceramic spheres to be used).

The silicone oils used in previous Spacelab experiments were rejected, because their solidification is ill defined and takes place at low temperature, while other frequently

used liquids (cyclohexane, cyclohexanol and other alcohols) were discarded because of their high volatility. In the end, water was chosen as the most suitable working liquid.

It was known that the tracers did not dissolve so well in water as in the silicone oils (the tracers have a tendency to clog and stick to the walls of the reservoir), but this problem was solved by placing them at the mouth of the feeding tube, separated from the stored liquid by a filter. In this way, the tracers could be added to the liquid during the formation of the liquid column by liquid injection.

It was also known that water is easily contaminated, introducing large uncertainties in surface-tension values. Trials were performed directly with the flight hardware to check the effect of water contamination by the vaseline used in the seals. A stable value of some 0.065 N/m for the surface tension of (contaminated) water was reached after several days of storage.

The fact that water expands by about 10% as it freezes was deemed to be irrelevant to the preparation of this experiment.

Ground experiments with millimetric zones on the freezing of drops³ and liquid bridges of water showed that the receding contact angle for solidification of water was near zero (calling for more precise configurations than the one intended here for microgravity conditions).

A striking effect was detected during the observation of the freezing of millimetric liquid zones: when the temperature of the solid support falls below 0°C, an opalescence quickly appears in the first few millimetres of liquid; it lasts for some seconds and then disappears while the solidification front continues to advance within that region. This effect, which we call 'surface opalescence', may be due to droplet formation at the free surface of the water (by water-vapour condensation from the surrounding air), or to a free-surface undercooling independent of the outside atmosphere. As its behaviour was not predictable during the ground trials, it was attributed to uncontrolled contamination in these millimetric liquid masses.

All the ground trials on liquid bridges were performed with liquid nitrogen as the cooling agent (because it was readily available). It was applied to one end of a long aluminium rod, 5 mm in diameter, the other end being the support of the liquid bridge. No significant differences were found between upward and downward solidification.

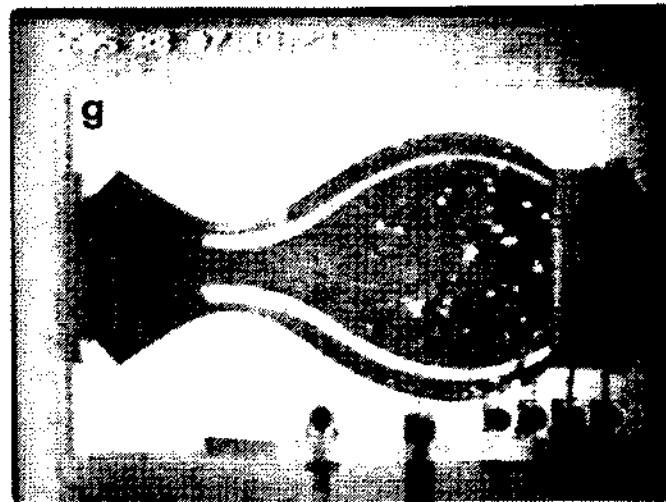
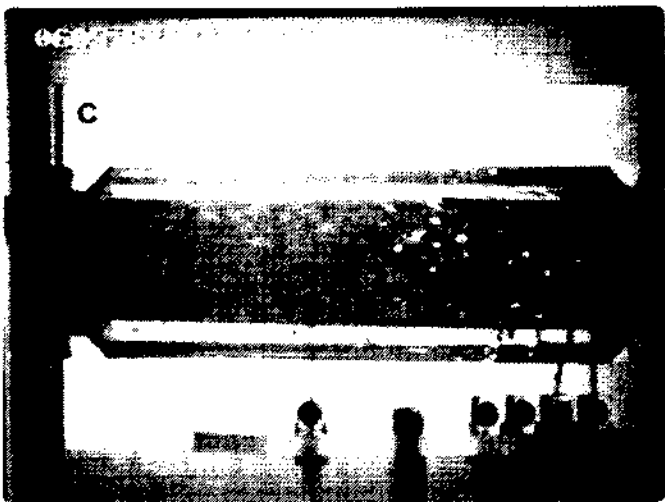
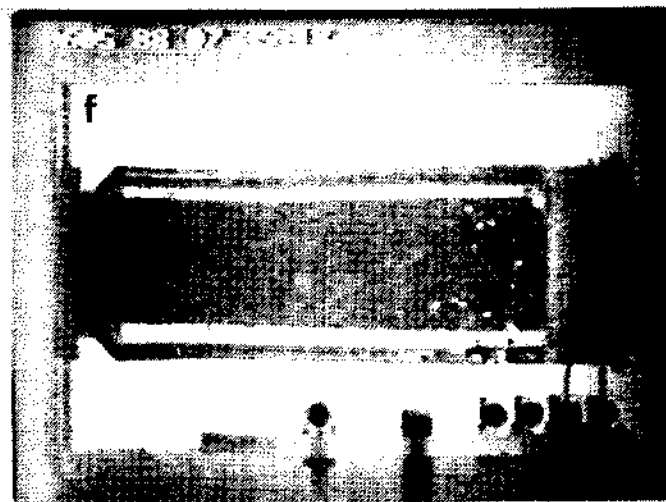
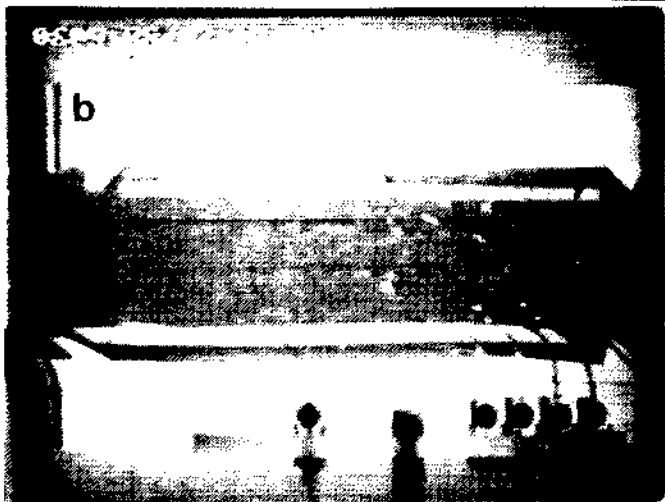
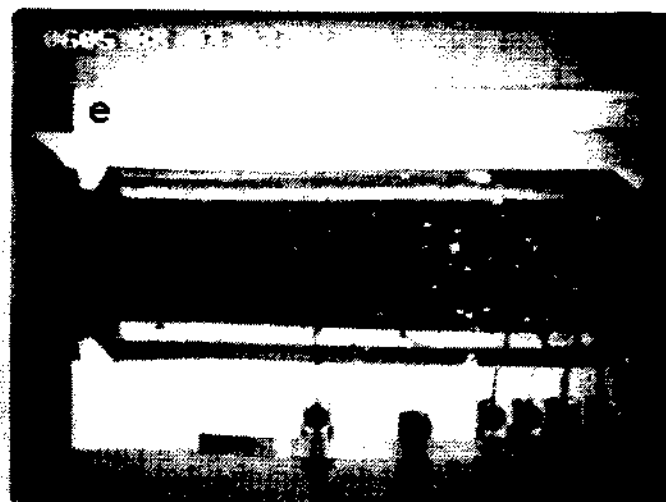
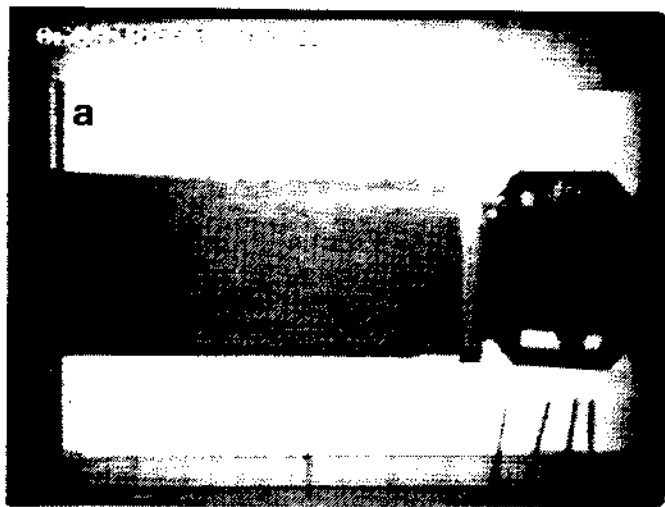
The flight hardware employed was the same liquid-column cell (LCC)⁴ that had been built by ERNO and already flown on Texus-12; it had, however, been modified slightly to incorporate the cooler, laser illumination and some thermocouples. In order to facilitate the analysis of the post-flight data (edge extraction and tracer motion), a video recording was needed (to automate image analysis) instead of the 16-mm film used on Texus-12. It is worth mentioning the controversy that arises with the image recording of experiments of this kind^{5,6}: video is more reliable and may reveal more detail than film, since, although film has a higher spatial resolution, video often has a higher temporal resolution than low-speed film.

In addition, a meridian light blade (enabling the tracers to be seen by reflection) was used. The resulting low-intensity image is then better matched with the videocamera, which records both this meridian-plane tracer motion and the background shadow of the liquid's free surface and solidification front.

Thermal diagnosis is provided by three thermocouples in the cooling disc (two of them used as a heat meter) and a comb carrying five thermocouples inserted radially in the axis of the liquid column (once established), at 2, 5, 9, 17 and 50 mm from the cooling disc. (The thermocouple nominally located at 2 mm appears, after the temperature recording, to be closer to the 3 mm point than to the 2 mm one (the wires are 0.5 mm thick).

The initial proposal to ESA was for experiment time aboard Spacelab-D2, but the Challenger accident prompted us to look for alternative experiment time aboard a Texus sounding rocket. The one hundred minutes of crystal growth originally foreseen had to be reduced to the 6 min capability of Texus, but the expected growth

3. Results of the flight experiment



in a 13 mm-long ice crystal was nevertheless deemed acceptable for experiment validation (although the resolution in receding contact angle and solidification-front dynamics was compromised).

In June 1987, the experiment was finally selected to fly on Texas-18, scheduled for launch in May 1988 from Kiruna. After some ground tests with the flight hardware using a simulated liquid column (a burette with water placed on top of the cooling disc) and a final verification at the launch site, a successful flight eventually took place on 6 May.

All data (video images, scientific and housekeeping data) were transmitted to ground in real time and everything worked as expected (Figs. 2, 3). As soon as the experimenters started to look at the information, however, a number of problems appeared, the most crucial being that the image transmission had seriously downgraded the quality of the video recording, adding some flickering and image distortion that prevent simple, automated image analysis. In addition, the contrast in the images is much poorer than ground-trial experience had led us to expect.

There were also several problems in the temperature recording. Firstly, the heat-meter data are unreliable (quick-look and final data do not match) and an out-of-range state occurred. In addition, the cooling law achieved (exemplified by the temperature of the disc) is not simple and not reproducible. An interesting 'kick' can be seen in the disc-temperature plot at about 260 K, perhaps due to initial undercooling of the liquid and subsequent release of the solidification enthalpy. However, the available diagnostics do not allow this to be clarified. The temperature variations at all thermocouple positions, and especially at the discs, before cooling started (from 50 to 140 s in Fig. 3) are also unexplained.

Another problem (expected) lies in the accelerometer readout which, just as on all earlier flights, shows mean residual levels of 10^{-2} g, while everybody knows (and the liquid-bridge stability demonstrates) that the actual value is well below 10^{-4} g. (In fact, in view of the greater cylindricity of the bridge aboard Texas, it must be much less than the 70×10^{-6} g computed from Spacelab-D1 data⁶).

One interesting finding is that the tracers are nearly quiescent, notwithstanding the fact that there should be some Marangoni convection due to the temperature gradient along the free surface, which is of the order of $10^\circ\text{C}/\text{mm}$ near the solidification front. The explanation may be that, in spite of the large variation in the surface tension of pure water with temperature, this effect is overridden by the presence of impurities.

It can also be seen from the images that the solidification front is planar, although it is not well defined (the visualisation system needs improving considerably in this respect). It can clearly be seen that, when the re-entry drag breaks the liquid bridge, the three-phase contact line remains attached to the corner of the growing crystal.

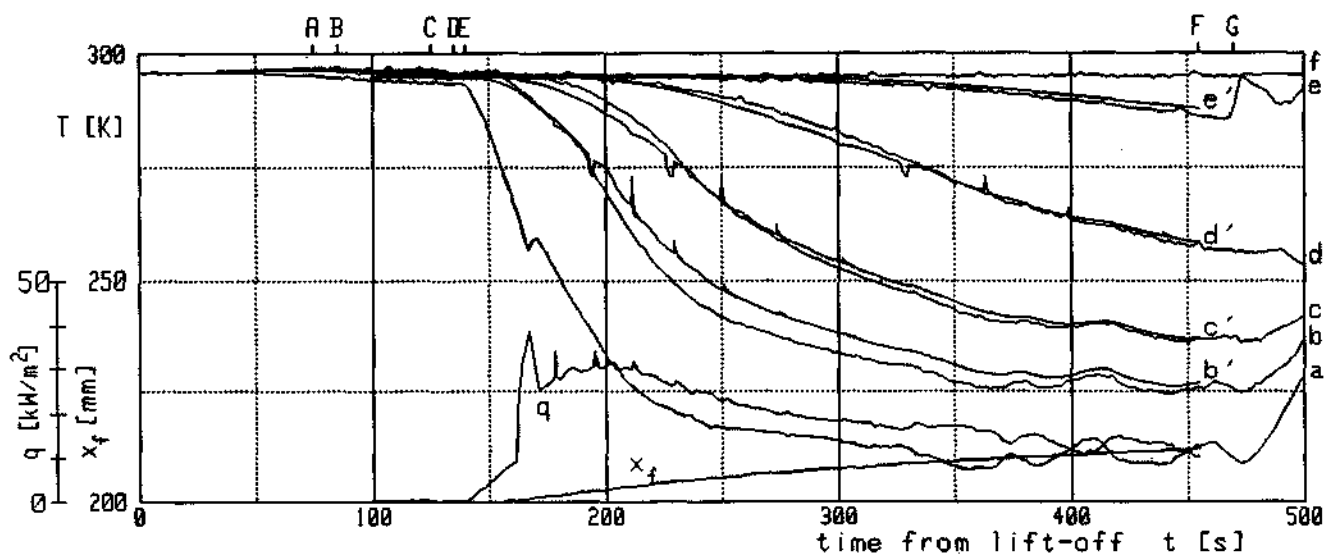
Although the microstructural analysis of the ice crystal grown was not of prime concern here, it may be important for future trials to start the growth at a single point

Figure 2. Selected video frames (time from lift-off):

- (a) 100 s, establishing the liquid column (at 2 mm/s)
- (b) 137 s, insertion of thermocouple comb into the liquid
- (c) 168 s, surface opalescence appears
- (d) 170 s, surface opalescence disappears
- (e) 183 s, ice crystal appears
- (f) 455 s, end of microgravity period (13 mm ice length)
- (g) 469 s, breakage of the liquid column (rocket reentry)
- (h) 480 s, broken bridge (a drop of water remains between the ice and the fourth thermocouple). The black band in the middle is a black slit in the background lighting to enhance visualisation

Figure 3. Evolution of selected temperatures, heat flux at the disc, and ice length.

- A. Start of microgravity period
- B. Start of column formation
- C. Insertion of thermocouple comb into the liquid
- D. Start of cooling
- E. Final column length attained
- F. End of microgravity period (re-entry)
- G. Column breakage; a, b, c, d, e, f: temperature measurements by the thermocouples at the disc and at 3, 5, 9, 17 and 50 mm from the disc, respectively; b', c', d', e': numerical temperature estimation at the corresponding location (assuming curve a as input); q: heat flux numerically computed from curves a and b; x_f : axial position of the solidification front



instead of at the whole disc face, in order to promote the formation of a single crystal (perhaps the receding contact angle is dependent on that).

On the other hand, numerical simulation with the thermal model, explained in the appendix, shows good agreement with experimental results (Fig. 3), except that the temperature profiles of the thermocouple readouts appear to fall (cool) later and more steeply than the one-dimensional thermal model suggests. Lateral heat input from the atmosphere could provide an explanation for the first effect, but not for the second.

4. Conclusions

The feasibility of establishing long liquid columns (86 mm by 30 mm diameter) quickly (in less than a minute) on a sounding rocket has been demonstrated. Predictions of the thermal behaviour of the system have been shown to be very accurate, with uncertainties of just a few percent (e.g. with regard to the length frozen in the time available).

The short solidification time that the Texus flight allows (5 min) is too restricted for the foreseen integral analysis to be performed on the solidified column. Moreover, the already known fact that the receding contact angle of water upon solidification is near zero cannot be examined more closely with the aid of this experiment.

The real-time video link greatly degraded the quality of the images. However, even if this were not so, the visualisation system still needs a lot of improvement if the solidification interface is to be more clearly resolved (this may be done with ground experiments). Further work should also be directed towards clarifying the suitability of water as the working fluid, towards developing a reproducible thermal cooling history, and towards triggering single-crystal growth.

Appendix: The thermal model

The following properties for water are considered:

— freezing temperature	$T_f = 273 \text{ K}$
— solidification enthalpy	$h_f = 0.33 \times 10^6 \text{ J kg}^{-1}$
— thermal capacity of liquid	$c_l = 4200 \text{ J kg}^{-1} \text{ K}^{-1}$
— thermal capacity of solid	$c_s = 2000 \text{ J kg}^{-1} \text{ K}^{-1}$
— thermal conductivity of liquid	$k_l = 0.6 \text{ W m}^{-1} \text{ K}^{-1}$
— thermal conductivity of solid	$k_s = 2 \text{ W m}^{-1} \text{ K}^{-1}$
— density of ice	$\rho_s = 920 \text{ kg m}^{-3}$

One-dimensional behaviour is assumed (because the aluminium disc can be assumed to be isothermal, the surrounding air adiabatic, the receding contact angle $\gamma \approx 0$, and the increase in volume due to the frozen length negligible).

For the first-order estimation, the liquid column may be assumed to be initially at $T_f = 0^\circ\text{C}$ and the cooling disc brought suddenly to $T_d = -60^\circ\text{C}$ (the nominal disc temperature selected). Equating the heat withdrawal through the ice length x_f to the heat release by solidification,

$$k_s \frac{T_f - T_d}{x_f} = \rho_s h_f \frac{d x_f}{d t}$$

we obtain the approximated solidification front position as a function of time:

$$x_f = \sqrt{\frac{2 k_s (T_f - T_d)}{\rho_s h_f} t}$$

which gives $x_f = 14 \text{ mm}$ for the 5 min of crystal growth (6 min of microgravity provided by Texus, minus 1 min of column formation). The growth rate dx_f/dt at the end of the 5 min period is about 1.5 mm/min , and the heat flux at the disc,

$$q = \sqrt{\frac{\rho_s h_f k_s (T_f - T_d)}{2 t}}$$

is about 8 kW m^{-2} .

For the finer analysis, a one-dimensional discrete thermal model was numerically simulated, the enthalpy method being used to cope with the freezing-front problem. A constant-width mesh with $\Delta x = 1$ mm was used to generate the plot in Figure 3 using the explicit form of the discretised heat equation

$$\rho \Delta x \frac{h^+(I) - h(I)}{\Delta t} = k_+ \frac{T(I+1) - T(I)}{\Delta x} - k_- \frac{T(I) - T(I-1)}{\Delta x}$$

where ρ must be assumed constant (we put $\rho = \rho_s$), Δt is selected appropriately small to keep the explicit scheme stable, I is the axial node ($I=0, 1, \dots, 86$ for the 86 mm-long column and a $\Delta x = 1$ mm), k_+ and k_- are the thermal conductivities to the right and left of the I node (to be chosen from that of water or ice according to the temperature), and T , the temperature at the nodal points, is computed from the following equation of state:

$$T(h) = \begin{cases} h/c_s & \text{if } 0 \leq h \leq c_s T_f \\ T_f & \text{if } c_s T_f \leq h \leq c_s T_f + h_f \\ T_f + \frac{h - c_s T_f - h_f}{c_l} & \text{if } h > c_s T_f + h_f \end{cases}$$

Thus, if we start with $h(I) = c_s T_f + h_f + c_l (T_i - T_f)$ for all I nodes (T_i is the initial ambient temperature), the scheme permits successive computations of $h(I)$ for all times as a function of the material properties and the boundary conditions [$T(0)$ and $T(86)$]. To obtain the plot shown in Figure 3, it was assumed that

$$T_i = 295 \text{ K and } T(0) = T_d(t),$$

where $T_d(t)$ has been input from the flight data.

In addition, a small refinement was also introduced into the model to approximate the temperature profile better in the cell where the solidification front happens to lie, as a function of time. With the above model, the temperature at this nodal point will stay at T_f as long as the front x_f is within this cell (moving from one end to the other). The refinement consisted of first locating x_f within the cell, assigning T_f at this point, and then computing the temperature at the centre of this cell (at the nodal point) by linear interpolation.

The small spikes that appear on the numerical simulation shown in Figure 3 are spurious, and are due to discontinuities when the front changes from one cell to the other, but no further refinement was deemed necessary.

1. Martínez I & Eyer A 1986, Liquid bridge analysis of silicon crystal growth experiments in Spacelab-1, *J. Crystal Growth*, **75**, pp. 535–544.
2. Sanz A 1986, The crystallization of a molten sphere, *J. Crystal Growth*, **74**, pp. 642–655.
3. Sanz A, Meseguer J & Mayo L 1987, The influence of gravity on the solidification of a drop, *J. Crystal Growth*, **82**, pp. 81–88.
4. Martínez I & Sanz A 1985, Long liquid bridges aboard sounding rockets, *ESA Journal*, **9**, pp. 323–328.
5. Martínez I 1984, Liquid column stability, ESA Special Publication SP-222, pp. 31–36.
6. Martínez I 1986, Stability of long liquid columns in Spacelab-D1, ESA Special Publication SP-256, pp. 235–240.

References